Thermo-Mechanical and Adhesive Properties of Polymeric Films Based on ZnAl-Hydrotalcite Composites for Active Wound Dressings

Luana Perioli,[1] Andrea Dorigato ,[2] Cinzia Pagano,[1] Matteo Leoni,[3] Alessandro Pegoretti[2]
[1]*Department of Pharmaceutical Sciences, University of Perugia, Perugia 06123, Italy*
[2]*Department of Industrial Engineering and INSTM Research Unit, University of Trento, Trento 38123, Italy*
[3]*Department of Civil, Environmental and Mechanical Engineering, University of Trento, Trento 38123, Italy*

Composite films based on sodium carboxymethyl cellulose (Na-CMC) loaded with a ZnAl$(OH)_2CO_3{\cdot}yH_2O$ hydrotalcite (ZnAl-HTlc), were developed and characterized. The composites were mechanically more stable than the matrix alone: the noticeable enhancement of elastic modulus, creep resistance and failure properties, all proportional to the filler content, came at the expenses of a certain embrittlement. The filler tended to aggregate in the composites and the size of the aggregates increased with ZnAl-HTlc amount. Contact angle measurements highlighted how ZnAl-HTlc introduction in the polymeric matrix could strongly modify the wettability conditions of the films increasing their hydrophilicity. Bioadhesion tests showed that the adhesion behavior of the composites decreased as ZnAl-HTlc amount increases, testifying the influence of the filler on the ability of the film to bind skin surface. Therefore, the developed films may find application as active wound dressings since ZnAl-HTlc can be easily intercalated with an active pharmaceutical ingredient to be progressively released on the wound. POLYM. ENG. SCI., 59:E112–E119, 2019. © 2018 Society of Plastics Engineers

INTRODUCTION

Polymers currently find many applications in the pharmaceutical field as fillers, binders, disintegrant, gliding, swelling, suspending, emulsifiers, flocculating agents, and so forth [1]. Polymers are usually employed for their biocompatibility, permeability, hydrophilicity, and low coefficient of friction [2]. Hydrophilic polymers are able to swell (up to 90%) in contact with water forming hydrogels useful for different applications in drug delivery, stem cell engineering, immunomodulation, cellular and molecular therapies, wound healing [2, 3]. Among the numerous polymers available, sodium carboxymethyl cellulose (Na-CMC) is one of the election polymers used in pharmaceutical field because of its exceptional properties such as high viscosity, transparency, hydrophilicity, nontoxicity, biocompatibility, biodegradability, and good film forming ability. This latest feature has allowed the development of various cellulose-based devices. Chemically, Na-CMC consists of β-linked glucopyranose residues with different levels of Na-carboxymethyl ($-OCH_2COO^-Na^+$) substitution. As three hydroxyls are present per C_6 ring, the maximum degree of substitution is three [4]. In general, cellulose derivatives are environmentally friendly and therefore favorable in the health field, as they can be easily digested or metabolized by those microorganisms present in air, water and soil able to synthesize cellulose-specific enzymes [5]. All these properties make Na-CMC a suitable material for the development of wound dressings. The main limiting factor of Na-CMC for this application is represented by the low mechanical properties [6]: the integrity of the formulation could be impaired before, during and after the application. In this way, wound dressing effectiveness and patient compliance are compromised [7]. A possible solution to overcome these limits is to add nanoparticles (<10% w/w) to the polymer matrix, to form a nanocomposite. An improvement of the mechanical, thermal and gas barrier properties is expected [8, 9]. Among the large number of available fillers, layered double hydroxides (HTlcs) find interesting application in the pharmaceutical field. HTlcs, anionic clays or hydrotalcites (from the name of the most important mineral belonging to this family) have a general formula $M(II)_{1-x}M(III)_x(OH)_2(A^{n-})_{x/n}{\times}yH_2O$, where M(II) is a divalent cation, M(III) is a trivalent cation and A^{n-} is a n-valent interlayer anion specie. The interlayer anions can be easily exchanged for other inorganic or organic species, thus transforming the HTlc into drug carriers and drug-release materials both for oral and topical use [10–14].

Biohybrids of HTlc and biomolecules can be designed to carry or drop functional biomolecules in gene therapy and drug delivery [15]. Many studies demonstrated their ability to form micro- and nanocomposites with improved mechanical properties [16, 17]. Nanocomposites based on Na-CMC and HTlcs have already been proposed in the literature, but only a few examples exist. Yadollahi et al. [18] observed that HTlc increases the mechanical properties of Na-CMC-based films. This gain can be attributed to the strong interfacial adhesion of HTlc with Na-CMC [19–21].

The aim of this work is to study the impact of the physical dispersion of HTlc on the morphological and structural properties of composite films made of Na-CMC and ZnAl-$(OH)_2CO_3{\cdot}yH_2O$ (ZnAl-HTlc). For shortness the composite films will be here called CMC-HTlc. The films were characterized from morphological (X-ray diffraction [XRD], contact angle measurements, field emission scanning electron microscope [FESEM]), thermal (differential scanning calorimetry [DSC]) and a mechanical (quasi-static tensile tests, creep and recovery tests) points of view. Bioadhesion tests were also performed. The developed CMC-HTlc composites could be used for patches that can simultaneously protect the skin and provide a controlled drug release. Drug loading and delivery properties are promising and detailed studies are in progress.

EXPERIMENTAL

Materials

A purified granular Na-CMC (BLANOSE Cellulose Gum), was supplied by Hercules Inc. (Wilmington, DE). On the basis

Correspondence to: A. Dorigato; e-mail: andrea.dorigato@unitn.it
DOI 10.1002/pen.24877
Published online in Wiley Online Library (wileyonlinelibrary.com).

TABLE 1. Composition of the starting solutions from which the films were obtained.

Sample	Glycerol (wt%)	Na-CMC (wt%)	HTlc (wt%)	water (wt%)	HTlc in dried films (wt%)
CMC2	10.0	2.0	0.0	88.0	0.0
CMC2-HTlc1	10.0	2.0	1.0	87.0	4.1
CMC2-HTlc1.5	10.0	2.0	1.5	86.5	7.3
CMC2-HTlc2	10.0	2.0	2.0	86.0	8.5
CMC2-HTlc3	10.0	2.0	3.0	85.0	11.1

of the producer datasheet, the material had a degree of substitution of 0.65–0.90 and an apparent density range of 0.55–1.00 g/cm^3. Glycerol (melting point 18°C, density 1.26 g/cm^3, molecular weight 92.1 Da) was purchased from ACEF Spa (Piacenza, Italy). The ZnAl-HTlc compound was synthesized via co-precipitation following a well-established literature procedure [22]. Deionized water was obtained by reverse osmosis process in a MilliQ system supplied by Millipore (Rome, Italy). Other reagents and solvents were of reagent grade and were used without further purification.

Preparation of the Polymeric Films

The films were prepared via solvent casting method [23]. Hydrogels were prepared at room temperature as follows: ZnAl-HTlc powder was dispersed in water and sonicated for 10 min. After this time glycerol was added to the dispersion and lastly CMC. The polymer was dispersed slowly in order to obtain a uniform hydration and to prevent lumps formation. In order to remove air, the hydrogel was kept under magnetic stirring (600 rpm), at room temperature, under vacuum for 24 h. The obtained hydrogels were then poured into cylindrical silicone molds (4 cm in diameter) and heated at 37°C under vacuum for 24 h. The samples were named according to polymer and filler concentration. For instance, CMC2-HTlc1.5 designates the composite film prepared from solutions containing 2 wt% of Na-CMC and 1.5 wt% of ZnAl-HTlc, respectively. Table 1 lists the composition of the hydrogels employed for the casting of the films together with the actual ZnAl-HTlc content in the dried film determined from the mass residue at 700°C. The latter was found via thermogravimetric tests performed under nitrogen atmosphere.

In order to observe the effect of humidity on the mechanical properties (i.e., tensile and creep properties) two set of film samples were kept at room temperature at two different humidity conditions: 30% RH (in a desiccator with silica gel) and 50% RH (in a desiccator with a $Mg(NO_3)_2{\cdot}6\ H_2O$ solution), characterized by a solubility of 1.25 g/mL that guarantees the desired humidity content).

Experimental Techniques

Bulk, Surface, and Morphology Characterization. XRD patterns of starting powders and films (30% RH-conditioned samples) were collected on a high-resolution Philips X'Pert MRD diffractometer equipped with a Cu tube operated at 40 kV and 45 mA, the patterns were collected in the 2–70° 2θ range with a step of 0.05° to ensure the 001 reflections were fully included.

In order to evaluate the surface properties (i.e., wettability) of the prepared films, contact angle was measured trough a Wilhelmy balance testing apparatus. A thin vertical sample was brought in contact with the liquid and the change in its weight was detected through a balance. The force (F) detected by the Wilhelmy balance is a combination of buoyancy and wetting force. It was therefore possible to evaluate the contact angle θ by the *Eq. 1*:

$$F=\gamma_{lv}p\cos\theta-V\Delta\rho g \quad (1)$$

Where γ_{lv} is the liquid surface tension, p is the wetted perimeter, V is the volume of the displaced liquid, $\Delta\rho$ is the difference in density between the liquid and air, and g is the acceleration of gravity [24]. As the solid sample is pushed into or pulled out of the liquid, an advancing (θ_a) or receding (θ_r) contact angle could be, respectively, established. Both the matrix (CMC2) and the CMC2-HTlc3 composites (30% RH-conditioned samples) were tested with this technique. The fracture surface of the nanocomposite films (30% RH-conditioned samples) was observed with a Zeiss Gemini Supra 40 FESEM; the samples were fractured using liquid nitrogen and then electrically connected to the microscope stub using silver paste.

Thermo-Mechanical Properties. DSC tests were performed on 30% RH-conditioned samples by using a Mettler Toledo DSC30 machine. Each sample was put in aluminum crucibles with a volume of 40 μL and tested under a nitrogen flow of 150 mL/min, heating/cooling rate of 10°C/min. Two consecutive heating cycles from −50 upto 180°C were performed. In the first cycle the presence of water can be identified, whereas in the second one the glass transition temperature (T_g) of the Na-CMC matrix can be better measured.

Quasi-static and creep tests were conducted on rectangular film samples (5 mm wide and 0.384 ± 0.003-mm thick) using an Instron 4502 electromechanical testing machine equipped with a 10 N load cell. Quasi-static uniaxial tensile test were performed at a constant crosshead speed of 10 mm/min, with a span length of 20 mm. For each sample, the secant elastic modulus at deformation of 5% ($E_{5\%}$), 25% ($E_{25\%}$), and 50% ($E_{50\%}$) were determined. Moreover, the stress and the strain at break (σ_b and ε_b, respectively) were computed. At least five specimens were tested per sample.

For the creep tests, a constant stress corresponding to 20% of the σ_{max} of the CMC2 sample (i.e., 0.29 MPa for the 30% RH samples and 0.17 MPa for the 50% RH samples) was applied

TABLE 2. Data for the starting powders and films: basal peak positions and basal spacing (interlayer distances) from XRD analysis, T_g from DSC tests and mean size of the aggregates from microscopy.

Sample	Form	Basal peak position (°)	Interlayer distance (Å)	T_g (°C)	Mean size of aggregates (μm)
HTlc	Powder	11.45	7.72	—	—
CMC2	Film	—	—	139.2	—
CMC2-HTlc1	Film	11.91	7.43	135.7	1.8 ± 0.2
CMC2-HTlc1.5	Film	11.76	7.52	132.7	3.2 ± 0.2
CMC2-HTlc2	Film	11.82	7.48	125.5	6.4 ± 0.3
CMC2-HTlc3	Film	11.67	7.58	124.1	6.8 ± 0.5

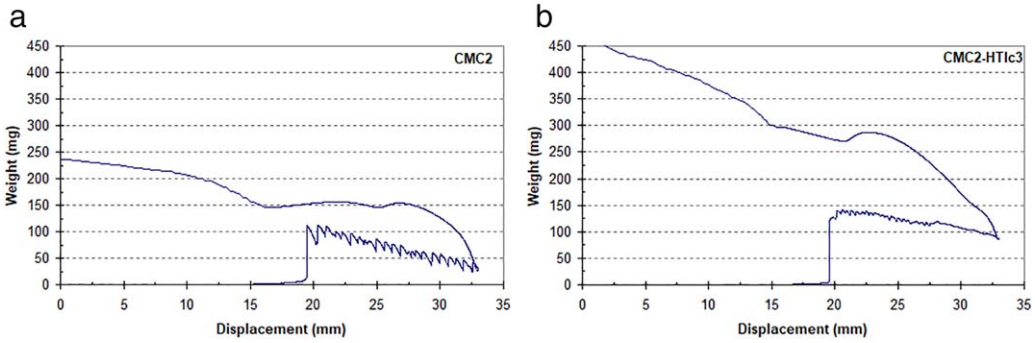

FIG. 1. Advancing/receding curves from dynamic contact angle measurements on (a) CMC2 and (b) CMC2-HTlc3 sample.

for 3,600 s. In this way, a time dependent creep compliance (obtained by dividing the creep deformation by the constant stress), was determined. After 3,600 s the load was removed keeping a constant strain level, and a recovery time of 3,600 s was chosen. A relaxation modulus, taken as the ratio between the time dependent stress and the constant deformation, was determined.

Bioadhesion/Hydration Tests. The bioadhesive features of the films (i.e., adhesion force and time) were evaluated on fresh pigskin substrates taken from Large White pigs (160–165 kg), supplied by the veterinary service of ASL N1 of Città di Castello (Perugia, Italy). The pig skin was kept at 4°C until its use. The bioadhesion force was measured by a Didatronic dynamometer (Terni, Italy). The polymeric films were glued with a cyanoacrylate glue to the punch. The pig skin was glued to the bottom of a sample holder placed in a thermostatic water bath at 32°C on the machine basement. Pig skin and films were wetted with 100 μL of buffer solution simulating healthy skin. A pressure was applied for 20 s to facilitate the adhesion between skin and film; a traction was then applied on the film to force deadhesion. When the film detached from the pig skin, the

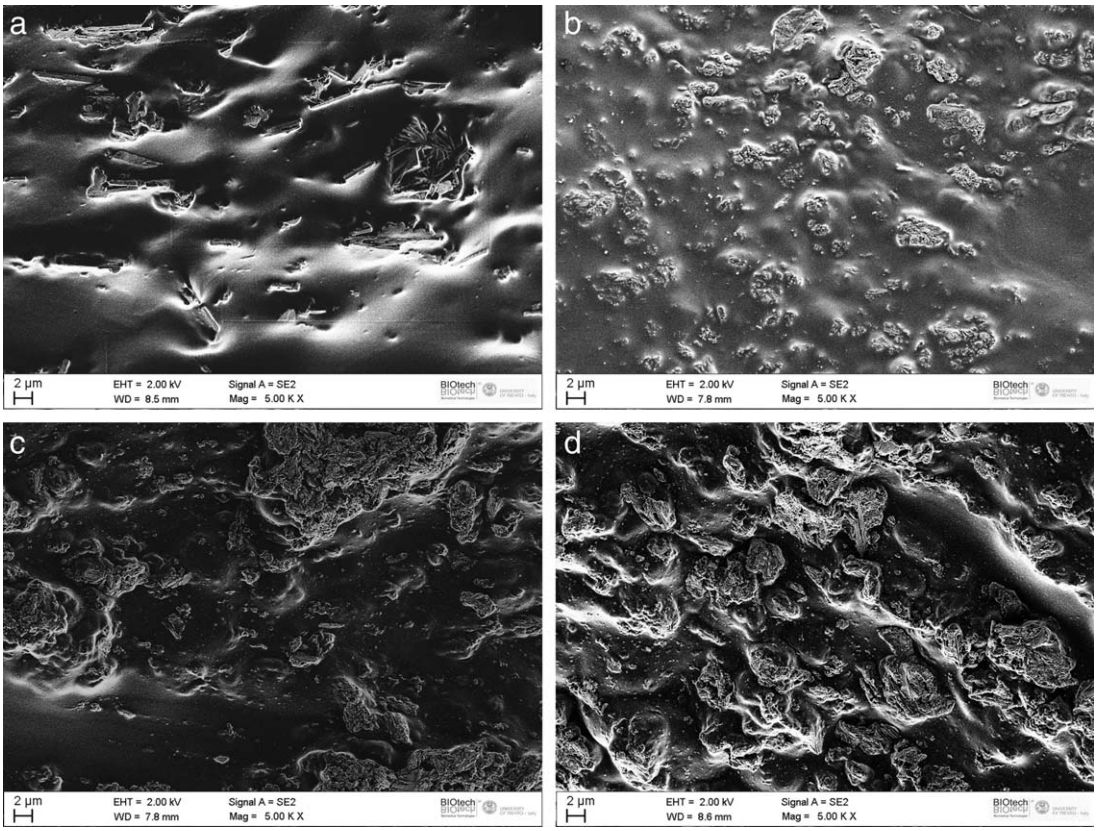

FIG. 2. FESEM micrographs of (a) CMC2-HTlc1, (b) CMC2-HTlc1.5, (c) CMC2-HTlc2, and (d) CMC2-HTlc3 samples (magnification 5,000×).

 DOI 10.1002/pen

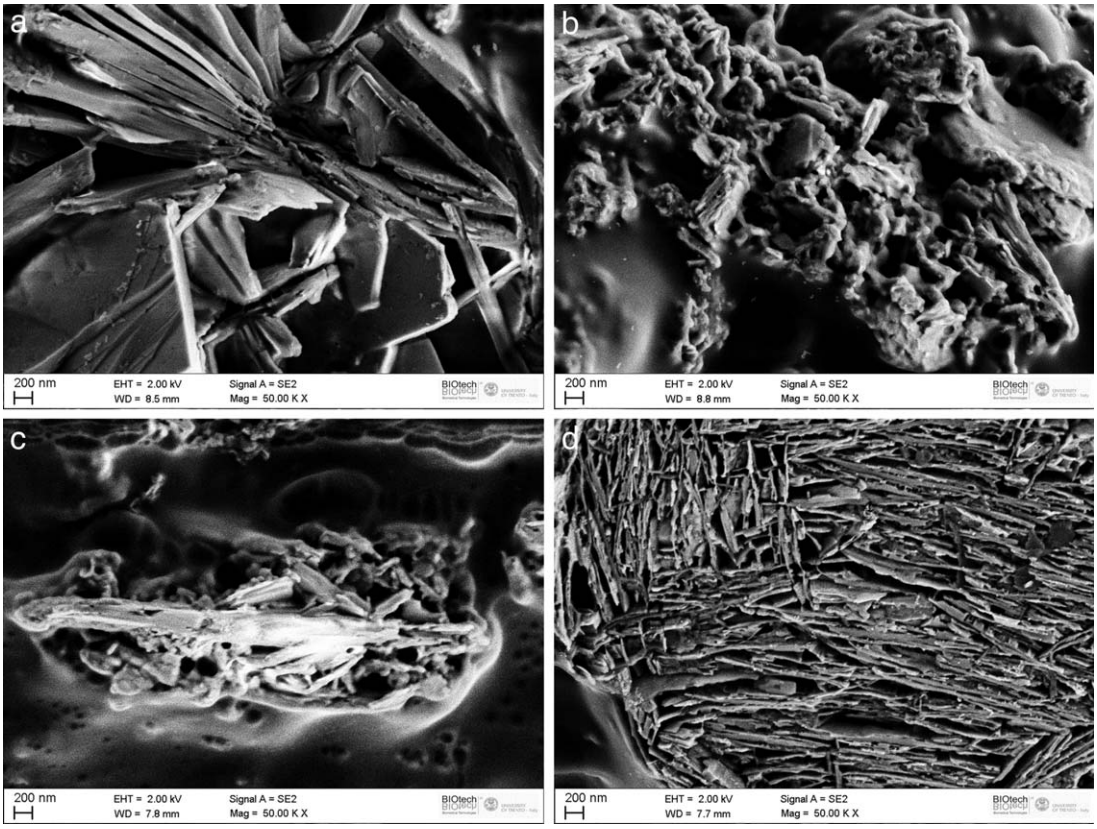

FIG. 3. FESEM micrographs of (a) CMC2-HTlc1, (b) CMC2- HTlc1.5, (c) CMC2- HTlc2, and (d) CMC2- HTlc3 samples (magnification 50,000×).

values of adhesion force were determined. The assay was carried out on circular disks with a diameter of 4 cm, and at least three specimens were tested for each sample. Two phosphate solutions were prepared with ultrafiltrated water: SOL1 containing 13.61 g of potassium dihydrogenphosphate (KH_2PO_4) in 1,000 mL of solution and SOL2 containing 35.81 g of anhydrous sodium hydrogen phosphate (Na_2HPO_4) in 1,000 mL. A phosphate buffer solution at pH = 5.5 (European Pharmacopoeia 9th Ed.) was then prepared by mixing 964 mL of SOL1 with 36 mL of SOL2.

RESULTS AND DISCUSSION

Morphological Characterization

The X-ray powder diffractgrams of the starting HTlc powder and of the various films were registered (graph not reported). The diffraction pattern of the ZnAl-HTlc powder showed the typical reflection of carbonate anion (7.7 Å) with the basal plane at $2\theta = 11.45°$. The broad bands observed in the pattern of CMC2 confirmed the completely amorphous nature of the Na-CMC. Table 2 summarizes the basal peak positions and the corresponding spacing of ZnAl-HTlc and of the films with various

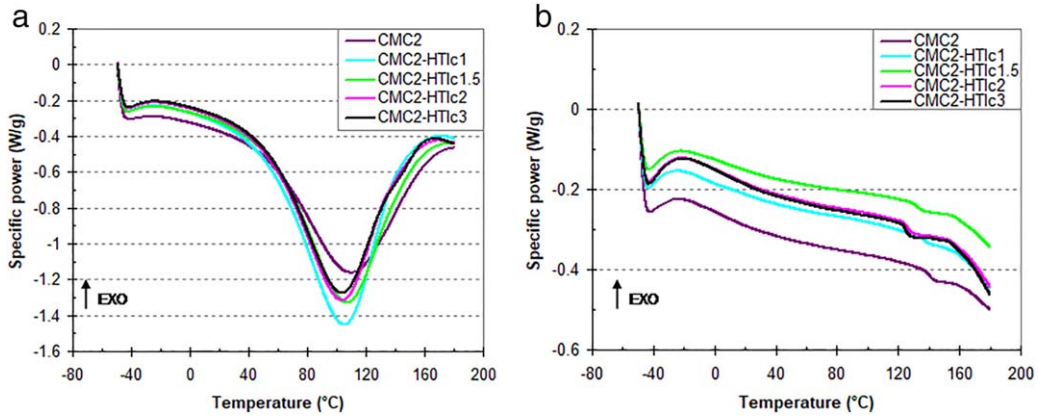

FIG. 4. DSC thermograms of CMC2 and relative composite films. (a) First heating stage and (b) cooling stage.

TABLE 3. Quasi-static tensile mechanical properties of the analyzed specimens in two humidity conditions.

Sample	$E_{5\%}$ (MPa)	$E_{25\%}$ (MPa)	$E_{50\%}$ (MPa)	σ_b (MPa)	ε_b (%)
RH 30%					
CMC2	0.13 ± 0.06	0.08 ± 0.01	0.07 ± 0.01	0.82 ± 0.18	486 ± 13
CMC2-HTlc1	0.14 ± 0.02	0.12 ± 0.01	0.13 ± 0.01	1.10 ± 0.05	201 ± 8
CMC2-HTlc1.5	0.27 ± 0.02	0.29 ± 0.01	0.39 ± 0.03	1.11 ± 0.18	136 ± 22
CMC2-HTlc2	1.91 ± 0.13	2.26 ± 0.16	2.23 ± 0.15	3.26 ± 0.26	124 ± 17
CMC2-HTlc3	5.42 ± 0.15	4.75 ± 0.23	4.18 ± 0.21	3.25 ± 0.19	82 ± 10
RH 50%					
CMC2	0.08 ± 0.01	0.06 ± 0.01	0.06 ± 0.01	0.56 ± 0.15	445 ± 35
CMC2-HTlc1	0.09 ± 0.02	0.06 ± 0.01	0.16 ± 0.01	0.55 ± 0.09	417 ± 40
CMC2-HTlc1.5	0.15 ± 0.02	0.12 ± 0.01	0.14 ± 0.02	0.92 ± 0.06	209 ± 25
CMC2-HTlc2	0.26 ± 0.04	0.26 ± 0.04	0.38 ± 0.06	1.64 ± 0.19	172 ± 12
CMC2-HTlc3	2.01 ± 0.05	2.33 ± 0.05	2.29 ± 0.09	2.74 ± 0.21	107 ± 6

ZnAl-HTlc amounts. The values of interlayer distance measured for all the films resulted similar to ZnAl-HTlc powder, testifying that not polymeric intercalation into ZnAl-layered double hydroxide (LDH) interlayer spaces occurred.

Contact angle measurements provide information about the hydrophilicity/hydrophobicity of the surface of the samples. Figure 1a and b shows the advancing-receding curves obtained from the Wilhelmy balance test done on the CMC2 and CMC2-HTlc3 samples. The advancing curves present a sawtooth shape, directly related to the peculiar structure of the Na-CMC. The material is initially hydrophobic, but in contact with water (polar) rearranges its chains, exposing the hydrophilic —OH groups to water and orienting the hydrophobic CH_3 inside the sample, thus becoming hydrophilic. When a new portion of non-wetted material is immerged in water, this chains rearrangement takes place and the initially hydrophobic CMC becomes hydrophilic. This kind of behavior is more evident in CMC2 than in CMC2-HTlc3: the LDH may therefore hinder the Na-CMC chain rearrangement. The CMC2 sample shows a higher advancing contact angle ($\theta_a = 43.1°$) and so it is more hydrophobic, while the CMC2-HTlc3 film, having a lower contact angle value ($\theta_a = 8.2°$), is more hydrophilic. Due to the irregular profile of the curves in the receding stage, it was not possible to determine the receding contact angle values. The surface behavior of the Na-CMC is therefore strongly influenced by ZnAl-HTlc addition.

FESEM micrographs were collected to evidence the filler distribution within the polymer matrix. In Fig. 2a–d it is possible to observe a homogeneous distribution of ZnAl-HTlc aggregates. The mean size of such aggregates increases with the ZnAl-HTlc content (cf. Table 2) most likely due to the initial increase in the viscosity of the mixture (related to the filler content) that makes it difficult to disperse the HTlc powder.

The Na-CMC seems unable to exfoliate the ZnAl-HTlc. The FESEM images of the composite films taken at a magnification of 50,000× (cf. Fig. 3a–d) show in fact lamellar structures of ca. 150–170 nm in thickness: considering a single lamella thickness of ca. 4.8 Å [25], the aggregates can be estimated to sum ca. 300 lamellae stacked together. We can expect a good interfacial adhesion between the filler and the polymer matrix, as the surface of the aggregates is surrounded by the polymeric matrix without voids or interfacial debonding. This feature could positively affect the mechanical behavior of the prepared materials.

Thermo-Mechanical Characterization

The DSC thermograms recorded in the first heating and in the cooling scans, are reported in Fig. 4a and b. In Fig. 4a, a big endothermic peak at about 100°C, whose origin is related to the evaporation of the water contained in the samples, can be observed. From the thermograms acquired during the cooling scan (Fig. 4b) the inflection point corresponding to the glass transition of the material can be estimated. The corresponding glass transition temperature (T_g) values are summarized in Table 2. It is interesting to observe that T_g decreases when increasing the ZnAl-HTlc content (from 139°C of the neat CMC up to 124°C for the CMC2-HTlc3 sample). Even if in literature it is often reported that the nanofiller introduction could slightly enhance the glass transition temperature of the materials [26] in some case the opposite trend was detected. For instance, in a paper of our group on cycloolefin copolymer/polyhedral oligomeric silsesquioxanes nanocomposites, a consistent T_g decrease upon nanofiller addition was found [27]. This result can be explained considering the formation of a mechanically compliant (soft) interphase between filler and polymeric matrix. In these conditions, the nanofiller behaves as a molecular lubricant agent within the matrix, and a certain fraction of macromolecules around the nanofiller surface can soften at lower temperature with respect to the unfilled matrix.

Quasi-static tensile tests have been carried out on both the 30% RH and on 50% RH-conditioned samples. From these tests we can evaluate the effect on the mechanical properties of both ZnAl-HTlc content and humidity. The most important quasi-static tensile mechanical properties of the films conditioned at RH of 30% and RH of 50%, are summarized in Table 3.

The secant elastic moduli at strain levels of 5% ($E_{5\%}$) 25% ($E_{25\%}$), and 50% ($E_{50\%}$) moderately increase up to a ZnAl-HTlc content of 1.5 wt% (in the hydrogel), and then abruptly increase for higher clay concentrations. For instance, an increase of 40 and 24 times of $E_{5\%}$ can be detected for the CMC2-HTlc3 composite at RH = 30% and 50%, respectively. The strong dependency of the material stiffness on filler aggregation was highlighted in recent articles of this group, in which a new theoretical model was proposed to model the elastic properties of particulate nanocomposites [28, 29]. According to our previous findings, filler aggregation may constrain a portion of matrix, thus limiting the mobility of macromolecules and providing a stiffening effect. A modification of the aggregative state of the

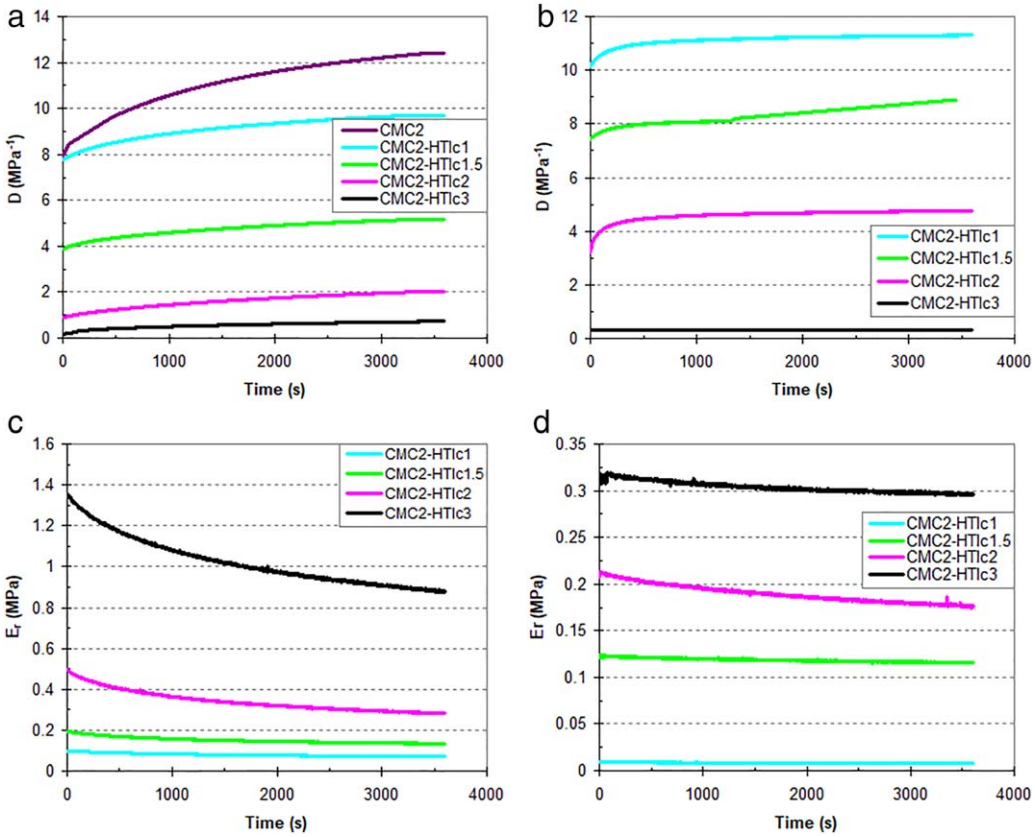

FIG. 5. Creep and recovery curves of the films. (a) Creep compliance and (b) recovery modulus of RH = 30% conditioned samples. (c) Creep compliance, and (d) recovery modulus of RH = 50% conditioned samples.

particles could therefore determine the enhancement of the elastic modulus observed in the tested materials. Even if some statistical deviations are associated to these measurements, at a general level it can be said that for the samples having the same filler amount the elastic modulus decreases with the strain level. Even if at room temperature all the prepared sample are well below their T_g, this result can be probably explained considering the viscoelastic relaxation phenomena present in all the polymer matrices. Moreover, stress at break values (σ_b) slightly increase up to a ZnAl-HTlc content of 1.5 wt%, then rapidly increase up to 2 wt% to finally stabilize to 3 wt%, probably because of the progressive filler aggregation. A σ_b increase of about four and five times can be detected for the CMC2-HTlc3 composite at RH = 30% and 50%, respectively. As frequently observed for filled systems [30], the strong filler aggregation evidenced in FESEM micrographs is responsible for a decrease of the strain at break (ε_b) for example, from 486% down to 82% in CMC2-HTlc3.

The 30% RH-conditioned samples have higher elastic moduli, maximum stress and stress at break values than the 50% RH-conditioned samples. The strain at break follows an opposite trend: this is likely due to the plasticizing effect of moisture. The aggregation of the clay at higher concentration can also lead to an inhomogeneous distribution: this can explain the higher standard deviation in the properties observed for the highly loaded films independent of the conditioning.

Figure 5 shows creep and recovery curves of the various films in both the analyzed RH conditions; the results are summarized in Table 4 in terms of creep compliance and relaxation

TABLE 4. Results of creep and relaxation tests on the analyzed specimens in two humidity conditions.

	RH = 30%		RH = 50%	
Sample	D (t = 3,600 s) (MPa^{-1})	E_r (t = 3,600 s) (MPa)	D (t = 3,600 s) (MPa^{-1})	E_r (t = 3,600 s) (MPa)
CMC2	12.42	—	—	—
CMC2-HTlc1	9.69	0.07	11.30	0.01
CMC2-HTlc1.5	5.14	0.13	8.89	0.11
CMC2-HTlc2	2.03	0.28	4.76	0.18
CMC2- HTlc3	0.74	0.87	3.28	0.30

TABLE 5. Adhesion force in phosphate buffer at pH 5.5.

Sample	Adhesion force (N)
CMC2	0.421 ± 0.130
CMC2-HTlc1	0.667 ± 0.085
CMC2-HTlc1.5	0.397 ± 0.036
CMC2-HTlc2	0.250 ± 0.027
CMC2-HTlc3	0.210 ± 0.044

modulus. Creep compliances are systematically higher in the 50% RH-conditioned samples than in the 30% RH-conditioned ones, because of the plasticizing effect played by the moisture within the material (see quasi-static tensile tests). In accordance with tensile tests, we observe a decrease in the creep compliance values at 3,600 s with increasing ZnAl-HTlc content, due to the stiffening effect of the filler. The Na-CMC sample at RH = 50% was unable to complete the creep test, thus indicating a limited intrinsic creep resistance of the hydrogel film. It is interesting to note that the relaxation modulus at 3,600 s increases with the filler amount. This result is in accordance with creep and tensile tests, and confirms the stabilizing effect of the filler. Considering the results of the quasi-static tensile tests, it can be concluded that the CMC2-HTlc2 sample is the formulation with the best balance of mechanical properties. In fact, it shows an interesting enhancement of the elastic modulus of the stress at break and of the creep stability, keeping the strain at break at an acceptable level.

Skin Adhesion Assay

Table 5 reports the results of the bioadhesion test performed in phosphate buffer at pH = 5.5 on 30% RH-conditioned samples, simulating practical conditions that can be found on the human skin. The skin surface is lipophilic, due to the high content of lipids in the stratum corneum [31]. According to contact angle measurements, in the absence of the ZnAl-HTlc the NaCMC chains reorganize when in contact with water, exposing the hydrophilic groups to the external surface and moving the hydrophobic groups to the inside, resulting in a hydrophilic surface with limited adhesion to skin.

The introduction of the filler turns the surface from hydrophobic to more hydrophilic. It can be observed that with a small quantity (1 wt%) an optimal effect is reached. The results coming from contact angle and bioadhesion tests suggest that, independently of all other possible purposes, ZnAl-HTlc is a cheap, non-toxic alternative to improve the properties (mechanical and adhesive) of Na-CMC. Bioadhesion studies on the CMC2-HTlc1 are promising for a practical application of the film on human skin. The adhesion results can be explained considering the steric hindrance of ZnAl-HTlc particles that reduces the contact between Na-CMC hydrophobic groups with skin, leading to a decrease in adhesion. Moreover, it can be hypothesized that the filler, hydrophilic in nature, produces modifications due to the establishment of weak interactions (e.g., hydrogen bonds) with the hydrophilic groups (—OH and C=O) of the polymer. Increasing the filler content increases the hydrophilic character of the film resulting in a low skin adhesion force. The 1 wt% of ZnAl-HTlc is probably able to engage the hydrophilic groups of NaCMC increasing the hydrophobic character of the film and thus its adhesion.

CONCLUSIONS

Composites based on NaCMC and ZnAl-HTlc intended for wound dressing applications were prepared and characterized. Even if the hydrogel is not able to intercalate the ZnAl-HTlc that remains in the film in an aggregated form, the filler has however still beneficial effects both on the mechanical and adhesion behavior of the films. In fact, a small addition changes the wettability and increases both the mechanical and adhesion properties. Higher quantities seem difficult to properly disperse and do not show practical advantages. Besides the possible pharmaceutical interest (as drug carrier), ZnAl-HTlc represents a suitable filler to improve the mechanical properties of films based on Na-CMC hydrogels. Further analyses on the drug release are in progress.

ACKNOWLEDGMENTS

Mrs Elena Tinazzo is gratefully acknowledged for her support to the experimental activity. The authors are very grateful to Mr Marco Marani and Mr Alfredo Casagranda for technical assistance.

REFERENCES

1. K.J. Gandhi, S.V. Deshmane, and K.R. Biyani, *Int. J. Pharm. Sci. Rev. Res.*, **14**, 57 (2012).
2. E. Caló, and V.V. Khutoryanskiy, *European Polymer Journal*, **65**, 252 (2015).
3. D. De Rossi, K. Kajiwara, Y. Osada and A. Yamauch, *Polymer Gels—Fundamentals and Biomedical Applications*, Plenum Press, New York (1991).
4. J. Li, R.B. Lewis, and J.R. Dahn, *Electrochem. Solid-State Lett.*, **10**, A17 (2007).
5. A. Sannino, C. Demitri, and M. Madaghiele, *Materials*, **2**, 353 (2009).
6. J.A. Stammen, S. Williams, D.N. Ku, and R.E. Guldberg, *Biomaterials*, **22**, 799 (2001).
7. J.S. Boateng, K.H. Matthews, H.N. Stevens, and G.M. Eccleston, *J. Pharm. Sci.*, **97**, 2892 (2008).
8. S. Pavlidou, and C.D. Papaspyrides, *Prog. Polym. Sci.*, **33**, 1119 (2008).
9. Y. Tanaka, J.P. Gong, and Y. Osada, *Prog. Polym. Sci.*, **30**, 1 (2005).
10. L. Perioli, and C. Pagano, *Exp. Opin. Drug Deliv.*, **9**, 1559 (2012).
11. L. Perioli, M. Nocchetti, P. Giannelli, C. Pagano, and M. Bastianini, *Int. J. Pharm.*, **454**, 259 (2013).
12. C. Pagano, M.C. Tiralti, and L. Perioli, *J. Pharm. Pharmacol.*, **68**, 1384 (2016).
13. L. Perioli, C. Pagano, M. Nocchetti, and L. Latterini, *J. Pharm. Sci.*, **104**, 3904 (2015).
14. L. Perioli, V. Ambrogi, B. Bertini, M. Ricci, M. Nocchetti, L. Latterini, and C. Rossi, *Eur. J. Pharm. Biopharm.*, **62**, 185 (2006).
15. P. Nalawade, B. Aware, V.J. Kadam, and R.S. Hirlekar, *J. Sci. Ind. Res.*, **68**, 267 (2009).
16. R. Charifou, F. Gouanvé, R. Fulchiron, and E. Espuche, *J. Polym. Sci. B Polym. Phys.*, **53**, 782 (2015).
17. L.Y. Jaramillo, J.C. Posada-Correa, E. Pabon-Gelves, E. Ramos-Ramırez, and N.L. Gutierrez-Ortega. Thermal and mechanical properties of nanocomposites based on polyethylene and Mg/Al hydrotalcite. *MRS Proceedings*, Vol. 1817, Cambridge University Press (2016).
18. M. Yadollahi, H. Namazi, and S. Barkhordari, *Carbohydr. Polym.*, **108**, 83 (2014).
19. H. Kang, G. Huang, S. Ma, Y. Bai, H. Ma, Y. Li, and X. Yang, *J. Phys. Chem. C*, **113**, 9157 (2009).
20. S. Huang, X. Cen, H. Zhu, Z. Yang, Y. Yang, W.W. Tjiu, and T. Liu, *Mater. Chem. Phys.*, **130**, 890 (2011).

21. F.K. Moreira, D.C. Pedro, G.M. Glenn, J.M. Marconcini, and L.H. Mattoso, *Carbohydr. Polym.*, **92**, 1743 (2013).
22. U. Costantino, F. Marmottini, M. Nocchetti, and R. Vivani, *Eur. J. Inorgan. Chem.*, **1998**, 1439 (1998).
23. L. Perioli, V. Ambrogi, F. Angelici, M. Ricci, S. Giovagnoli, M. Capuccella, and C. Rossi, *J. Control. Release*, **99**, 73 (2004).
24. Y. Yuan and T. R. Lee, "Contact angle and wetting properties", in G.. Bracco, B. Holst, *Surface Science Techniques*, Springer, Berlin (2013).
25. U. Costantino, A. Gallipoli, M. Nocchetti, G. Camino, F. Bellucci, and A. Frache, *Polym. Degrad. Stab.*, **90**, 586 (2005).
26. A. Dorigato, A. Pegoretti, L. Fambri, M. Slouf, and J. Kolarik, *J. Appl. Polym. Sci.*, **119**, 3393 (2011).
27. A. Dorigato, A. Pegoretti, and C. Migliaresi, *J. Appl. Polym. Sci.*, **114**, 2270 (2009).
28. A. Dorigato, P. Canclini, S.H. Unterberger, and A. Pegoretti, *Exp. Polym. Lett.*, **11**, 738 (2017).
29. A. Dorigato, Y. Dzenis, and A. Pegoretti, *Mech. Mater.*, **61**, 79 (2013).
30. A. Dorigato, and A. Pegoretti, *Polym. Eng. Sci.*, **57**, 537 (2017).
31. M. Horstmann, W. Müller and B. Asmussen, "Principles of skin adhesion and methods for measuring adhesion of transdermal systems", in E. Mathiowitz, E. C. Donald, III, and C.-M. Lehr, Eds. *Bioadhesive Drug Delivery Systems: Fundamentals, Novel Approaches, and Development*, *Chapter 8*, Marcel Dekker, New York (1999).